JOC*Article*

# Interaction of C−Si, C−Sn, and Si−Si σ-Bonds with Chalcogen Lone Pairs

Richard S. Glass,*,[†] Eric Block,[‡] Nadine E. Gruhn,[†] Jin Jin,[‡] Edward Lorance,[§]
Uzma I. Zakai,[†] and Shao-Zhong Zhang[‡]

*Departments of Chemistry, The University of Arizona, Tucson, Arizona 85721, University at Albany,
State University of New York, Albany, New York 12222, and Vanguard University,
Costa Mesa, California 92626*

rglass@u.arizona.edu

Received June 7, 2007
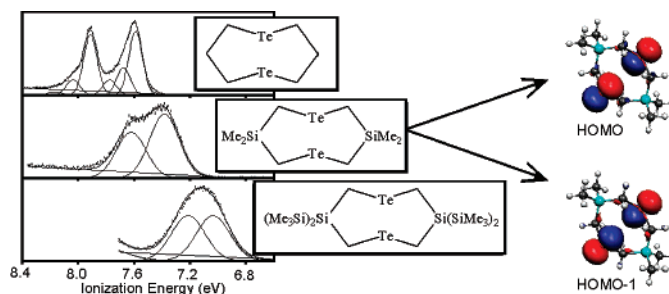
The ability of neighboring C−Si, C−Sn, and Si−Si groups in conformationally constrained cyclic molecules to reduce the lowest ionization energies of sulfur, selenium, and tellurium compounds has been determined by charge-transfer spectroscopy of complexes with tetracyanoethylene. For selected compounds, ionization energies were determined by gas-phase photoelectron spectroscopy. The lowest ionization energies measured by photoelectron spectroscopy, with one exception, correlate with the charge-transfer spectroscopic data. In addition, theoretical analysis has provided insight into the photoelectron spectra and the geometry-dependent interaction between C−Si or C−Sn bonds and chalcogen lone pairs. Substantial lowering of ionization energies is found which is anticipated to have important consequences in the chemistry of these and related species.

Introduction

It has been reported that carbocations[1] and, to a lesser extent, carbon radicals[2] are stabilized by β-silyl, germyl, and stannyl groups. Hyperconjugative resonance or σ−p overlap between the C−Si, C−Ge, or C−Sn bond and carbocations or carbon radicals is believed to account for this stabilization. Such an explanation requires appropriate geometry for orbital overlap, and this requirement has been observed experimentally. Analogous stabilization of heteroatom radical cations by β-silyl, germyl, and stannyl groups is expected. Indeed, there have been a few reports on the lowering of the oxidation potential of ethers,[3] amines,[3] and sulfides[4] appended with β-silyl or β-stannyl groups. Such lowered oxidation potentials are also reflected in lowered ionization energies determined by photoelectron spectroscopy (PES). To gain further insight into the effect of Si−

Si, C−Si, and C−Sn bonds on the ionization energy, oxidation potential, and redox chemistry of sulfur, selenium, and tellurium compounds, more than 40 new 4- to 12-membered heterocycles containing various combinations of Si or Sn together with S, Se, and Te were synthesized as reported elsewhere.[5] The β-Si−Si effect on the ionization of sulfides and selenides as determined by PES has been described elsewhere by us.[6] The

[†] The University of Arizona.
[‡] University at Albany.
[§] Vanguard University.

(1) (a) Bassindale, A. R.; Taylor, P. G. In *The Chemistry of Organic Silicon Compounds*; Patai, S., Rappoport, Z., Eds.; Wiley: Chichester, 1989; Part 2, pp 893−963. (b) Siehl, H.-U.; Müller, T. In *The Chemistry of Organic Silicon Compounds*; Rappoport, Z., Apeloig, Y., Eds.; Wiley: Chichester, 1989; Vol. 2, pp 595−701. (c) Lambert, J. B. *Tetrahedron* **1990**, *46*, 2677−2689. (d) Lambert, J. B.; Liu, X. *J. Organomet. Chem.* **1996**, *521*, 203−210. (e) Lambert, J. B.; Zhao, Y.; Emblidge, R. W.; Salvador, L. A.; Liu, X.; So, J.-H.; Chelius, E. C. *Acc. Chem. Res.* **1999**, *32*, 183−190. (f) Brook, M. A. *Silicon in Organic, Organometallic and Polymer Chemistry;* Wiley: New York, 2000. (g) Müller, T.; Margraf, D.; Syha, Y. *J. Am. Chem. Soc.* **2005**, *127*, 10852−10860. (h) Lambert, J. B.; Wang, G.; Teramura, D. H. *J. Org. Chem.* **1988**, *53*, 5422−5428. (i) Nguyen, K. A.; Gordon, M. S.; Wang, G.; Lambert, J. B. *Organometallics* **1991**, *10*, 2798−2803.

electrochemistry of selected examples from this series will be separately reported.[7] Here we report the lowest ionization energies of 27 of the new compounds as ascertained by charge-transfer (CT) spectroscopy of their tetracyanoethylene (TCNE) complexes. We also report previously unreported photoelectron spectra for many of these compounds, confirming assignments by theoretical calculations. The insights gained by these studies are relevant to the use of these compounds as metal ligands and electrically conducting materials (to be reported separately) and further support the conclusions of our earlier studies.[5,6]

Results and Discussion

Charge-Transfer Spectroscopy. Since a large number of new mixed group 14 and 16 heterocycles were on hand, an expedient method for determining their relative HOMO ionization energies was desired. This would provide a possible roadmap for predicting redox behavior. It has previously been reported that ionization energies may be obtained spectroscopically by measurement of the CT transition of TCNE complexes of alkyl and aryl derivatives of sulfur, selenium, and tellurium.[8] Consequently, the λ_{max} values of the CT complexes of the compounds synthesized in this study and TCNE were determined and are reported in Chart 1. If the ionization energy of the compound is too low (**2c, 3a−c**), then stable absorption spectra were not observed, presumably owing to electron transfer followed by fast decomposition.

Ionization energies are related to the CT transition of these complexes. Thus the second-order perturbation treatment of Mulliken shown in eq 1, where I_D is the ionization energy of the donor,

$$h\nu_{CT} = I_D - E_A - \frac{e^2}{r_{DA}} + P \qquad (1)$$

E_A is the electron affinity of the acceptor, r_{DA} is the mean separation of the donor and acceptor, and P is a second-order perturbation term, provides a means for obtaining ionization energies.[9] It is assumed that the last three terms in eq 1 are

(2) (a) Landais, Y. *C. R. Chimie* **2005**, *8*, 823−832. (b) Kawamura, T.; Kochi, J. K. *J. Am. Chem. Soc.* **1972**, *94*, 648−650.

(3) (a) Cooper, B. E.; Owen, W. J. *J. Organomet. Chem.* **1971**, *29*, 33−40. (b) Block, E.; Yencha, A. J.; Aslam, M.; Eswarakrishnan, V.; Luo, J.; Sano, A. *J. Am. Chem. Soc.* **1988**, *110*, 4748−4753. (c) Bock, H.; Meuret, J.; Stein, U. *J. Organomet. Chem.* **1990**, *398*, 65−77. (d) Bock, H.; Meuret, J. *J. Organomet. Chem.* **1993**, *459*, 43−54. (e) Yoshida, J.; Maekawa, T.; Murata, T.; Matsunaga, S.; Isoe, S. *J. Am. Chem. Soc.* **1990**, *112*, 1962−1970. (f) Yoshida, J. *Top. Curr. Chem.* **1994**, *170*, 39−81. (g) Yoshida, J.; Tsujishima, H.; Nakuno, K.; Isoe, S. *Inorg. Chim. Acta* **1994**, *220*, 129−135. (h) Yoshida, J.; Nishiwaki, K. *J. Chem. Soc., Dalton Trans.* **1998**, 2589−2596.

(4) (a) Glass, R. S.; Radspinner, A. M.; Singh, W. P. *J. Am. Chem. Soc.* **1992**, *114*, 4921−4923. (b) Glass, R. S.; Guo, Q.; Liu, Y. *Tetrahedron* **1997**, *53*, 12273−12286. (c) Li, H.; Nishiwaki, K.; Itami, K.; Yoshida, J. *Bull. Chem. Soc. Jpn.* **2001**, *74*, 1717−1725.

(5) (a) Block, E.; Dikarev, E. V.; Glass, R. S.; Jin, J.; Li, B.; Li, X.; Zhang, S.-Z. *J. Am. Chem. Soc.* **2006**, *128*, 14949−14961. (b) Block, E.; Glass, R. S.; Dikarev, E. V.; Gruhn, N. E.; Jin, J.; Li, B.; Lorance, E.; Zakai, U. I.; Zhang, S.-Z. *Heteroat. Chem.* **2007**, *18*, 509−515.

(6) Glass, R. S.; Block, E.; Lorance, E.; Zakai, U. I.; Gruhn, N. E.; Jin, J.; Zhang, S.-Z. *J. Am. Chem. Soc.* **2006**, *128*, 12685−12692.

(7) Evans, D. H.; Glass, R. S.; Block, E.; Macias-Ruvalcaba, N.; Okumura, N.; Zakai, U. I.; Jin, J.; Zhang, S.-Z. Manuscript in preparation.

(8) (a) Wagner, G.; Bock, H. *Chem. Ber.* **1974**, *107*, 68−77. (b) Glass, R. S.; Wilson, G. S.; Coleman, B. R.; Setzer, W. N.; Prabhu, U. D. G. *Adv. Chem. Ser.* **1982**, *201*, 417−441. (c) Frey, J. E.; Aiello, T.; Beaman, D. N.; Huston, H.; Lang, S. R.; Puckett, J. J. *J. Org. Chem.* **1995**, *60*, 2891−2901.
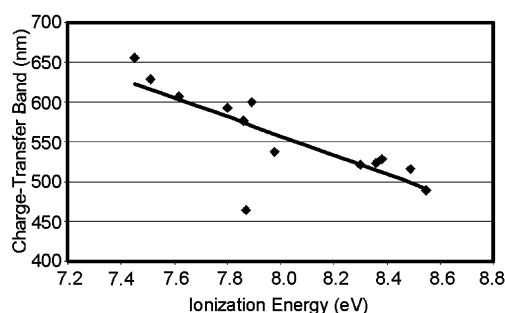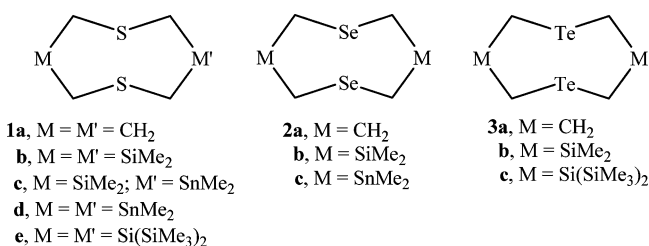
FIGURE 1. Plot of the ionization energy obtained by PES versus λ_{max} of the CT band with TCNE for all the compounds in Chart 1 for which both sets of data were measured.

constants, simplifying the expression to the linear equation shown in eq 2, where m and c are constants. In applying this method to the compounds studied here,
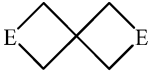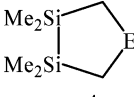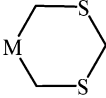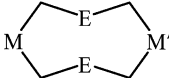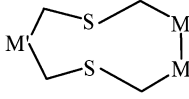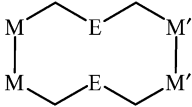
$$h\nu_{CT} = mI_D + c \qquad (2)$$

there are two concerns. In eq 1, there is a dependence on r_{DA}, which is assumed to be constant, but it is known that steric factors may cause this distance to vary. In addition, CT complexes between stannanes[10] and disilanes[11] with TCNE are known, but the consequences of having two complexation sites in one molecule are unknown. Consequently, the method was validated by comparing the ionization energy determined from the CT transition and the lowest ionization energy measured by PES. The ionization energies of the compounds for which photoelectron spectra have been measured are also given in Chart 1. A plot of PES ionization energy versus CT band maxima for those compounds for which both pieces of data are available is given in Figure 1. It should be noted that there is linear correlation between the ionization energies directly measured by PES and those calculated from the CT transition, thereby validating the method for this class of compounds. The one exception to the linear correlation is found for 3,3,4,4-tetramethyl-1,3,4-thiadisilolane, **4**, E = S. The R^2 from fitting these data points with a linear regression is 0.6117 but increases to 0.9274 if the data point for **4**, E = S is removed.

Photoelectron Spectroscopy and Theoretical Analysis. PES is an experimental technique that can be used to evaluate interactions of C−Si, C−Sn, and Si−Si σ-bonds on electron transfer from chalcogenides. This method provides a measure of the energy difference between radical cations and the corresponding neutral states, and the measured vertical ionization energies are generally discussed using Koopmans' theorem. Indeed, we have reported[6] the results of such analysis for several of the cyclic sulfides and selenides with Si−Si bonds whose charge-transfer bands λ_{max} are reported in Chart 1.

1a, M = M' = CH$_2$
b, M = M' = SiMe$_2$
c, M = SiMe$_2$; M' = SnMe$_2$
d, M = M' = SnMe$_2$
e, M = M' = Si(SiMe$_3$)$_2$

2a, M = CH$_2$
b, M = SiMe$_2$
c, M = SnMe$_2$

3a, M = CH$_2$
b, M = SiMe$_2$
c, M = Si(SiMe$_3$)$_2$

PES and theoretical analysis of a substantial number of additional compounds, not previously analyzed, are reported

CHART 1. Charge-Transfer Band Absorption Maxima of TCNE Complex[a] [λ_{max} (ϵ)] and Ionization Energies (eV) for Cyclic Sulfur, Selenium, and Tellurium Heterocycles

E = S[b]   478 (282); 8.71[c]
E = Se[d] 542 (266);   -

E = S   464 (183); 7.87[f]
E = Se 610 (137);   -

4

E = S, M = SiMe$_2$ 516 (111); 8.49[e]
E = Se, M = SiMe$_2$ 566 (234); -
E = S, M = Si(Me)tBu   520 (157); -
E = Se, M = Si(Me)tBu   574 (206); -
E = S, M = Si(SiMe$_3$)$_2$ 538 (348); 7.98[f]
E = Se, M = Si(SiMe$_3$)$_2$ 600 (299); 7.89[f]

M = CH$_2$ 498 (111); 8.55, 8.44[g]
M = SiMe$_2$ 572 (172);   -
M = Si(SiMe$_3$)$_2$ 592 (51);   7.80[f]
M = SnMe$_2$ 582 (266);   -

E = S,   M = M' = CH$_2$ (**1a**)   520 (125); 8.27[g]
E = Se, M = M' = CH$_2$ (**2a**)   584 (73); 8.00
E = S,   M = M' = SiMe$_2$ (**1b**)   584 (181); 7.90
E = Se, M = M' = SiMe$_2$ (**2b**)   638 (97); 7.71
E = S,   M = M' = Si(SiMe$_3$)$_2$ (**1e**)   628 (85); 7.51[f]
E = Se, M = M' = Si(SiMe$_3$)$_2$ 656 (44);   -
E = S,   M = SiMe$_2$, M' = SnMe$_2$ (**1c**) 622 (423); 7.66
E = S,   M = M' = SnMe$_2$ (**1d**)   -   7.50
E = Se, M = M' = SnMe$_2$ (**2c**)   -   7.42
E = Se, M = M' = CMe$_2$ 598;   -
E = Te, M = M' = CH$_2$ (**3a**)   -   7.59
E = Te, M = M' = SiMe$_2$ (**3b**)   -   7.38
E = Te, M = M' = Si(SiMe$_3$)$_2$ (**3c**)   -   7.04

M = M' = CH$_2$ 524;   8.36
M = SiMe$_2$, M' = CH$_2$ 576 (130); 7.85[f]
M = M' = SiMe$_2$ 592 (292); -
M = SiMe$_2$, M' = SnMe$_2$ 614 (552); -

E = S, M = M' = CH$_2$ 528;   8.38[g]
E = S, M = M' = SiMe$_2$ 608 (191); 7.61[f]
E = Se, M = M' = SiMe$_2$ 656 (374); 7.45[f]

[a] λ_{max} for the CT band for the TCNE CT complex
[b] Ref. 25.
[c] Ref. 26.
[d] Ref. 25, 27.
[e] Ref. 28.
[f] Ref. 6.
[g] Ref. 8b.

here. The photoelectron spectra for compounds **1a−e**, **2a−c**, and **3a−c** are shown in Figures 2−4, respectively, and the chalcogen lone-pair ionization energies measured are given in Table 1. The data for **1e** originally reported elsewhere[6] are reproduced here for ease of comparison. The photoelectron spectrum of **1a** has been reported previously[12] but was re-collected in this study under the same instrument conditions as the other compounds studied. The vertical ionization energy reported here for **1a** of 8.27 eV differs slightly from the previously reported value of 8.30 eV,[12] but the measured energy difference between the sulfur lone-pair ionizations is the same. The photoelectron spectra for **1a**, **2a**, and **3a** are very similar. In particular, there are two sharp peaks with some resolved vibrational structure at low ionization energies that are assigned in analogy with the previous assignments for **1a**.[12] Thus, these ionizations correspond to the antisymmetric and symmetric 3p, 4p, and 5p lone-pair orbitals for **1a**, **2a**, and **3a**, respectively. The antisymmetric lone-pair combination is the HOMO, and symmetric combination is HOMO-1. The ionization energies show the expected progression Te < Se < S.[13] Furthermore, the lone-pair splitting decreases in the order S (0.42 eV) > Se (0.35 eV) > Te (0.32 eV), indicating the lone-pair orbital overlap decreases in the order S > Se > Te.

Substitution of the 3,6-CH$_2$ moieties in the 1,5-dichalcogeno-canes by Me$_2$Si or Me$_2$Sn moieties results in dramatic changes

(9) (a) Foster, R. *Organic Charge-Transfer Complexes*; Academic: New York, 1969. (b) Mulliken, R. S.; Person, W. *Molecular Complexes*; Wiley: New York, 1969.
(10) (a) Gardner, H. C.; Kochi, J. K. *J. Am. Chem. Soc.* **1976**, *98*, 2460−2469. (b) Fukuzumi, S.; Kochi, J. K. *J. Phys. Chem.* **1980**, *84*, 608−616.
(11) (a) Traven, V. F.; West, R. *J. Am. Chem. Soc.* **1973**, *95*, 6824−6826. (b) Sakurai, H.; Kira, M.; Uchida, T. *J. Am. Chem. Soc.* **1973**, *95*, 6826−6827. (c) Tsutsui, S.; Takahashi, M.; Sakamoto, K. *Chem. Lett.* **2000**, 1376−1377.
(12) Setzer, W. N.; Coleman, B. R.; Wilson, G. S.; Glass, R. S. *Tetrahedron* **1981**, *37*, 2743−2747.

(13) Detty, M. R.; Logan, M. E. *Adv. Phys. Org. Chem.* **2004**, *39*, 79−142.
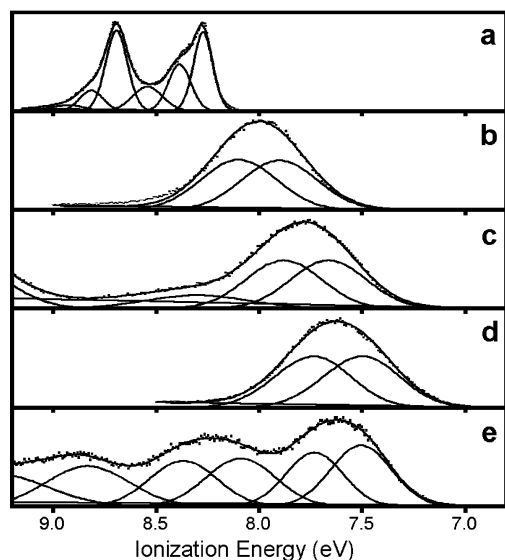
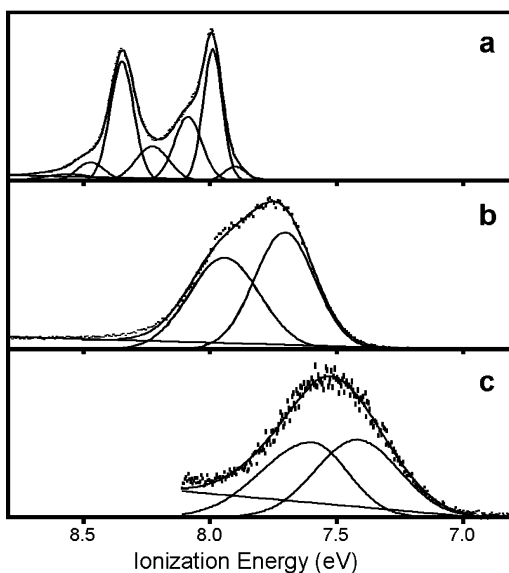**FIGURE 2.** He I photoelectron spectra of (a) **1a**, (b) **1b**, (c) **1c**, (d) **1d**, and (e) **1e**.

FIGURE 3. He I photoelectron spectra of (a) **2a**, (b) **2b**, and (c) **2c**.

FIGURE 4. He I photoelectron spectra of (a) **3a**, (b) **3b**, and (c) **3c**.

TABLE 1. Chalcogen Lone-Pair Ionization Energies for Compounds Studied Here by PES

compound	IE, eV	ΔIE
1a	8.27, 8.69	0.42
1b	7.90, 8.10	0.20
1c	7.66, 7.88	0.22
1d	7.50, 7.74	0.24
1e	7.51, 7.72	0.22
2a	8.00, 8.35	0.35
2b	7.71, 7.94	0.23
2c	7.42, 7.60	0.18
3a	7.59, 7.91	0.32
3b	7.38, 7.62	0.24
3c	7.04, 7.21	0.17

in their photoelectron spectra as enumerated below. The lone-pair ionizations of the Si- and Sn-substituted molecules are much broader, most likely because of the additional presence of low-frequency vibrational modes associated with the Si−C bonds, Sn−C bonds, or methyl substituents. Because both chalcogen lone-pair ionizations are broad and fall under one band with little or no structure, specific ionization energies are difficult to observe or precisely measure. The positions of the two ionizations listed for **1b−e**, **2b,c**, and **3b,c** are taken from a fit with two Gaussians constrained to similar intensities and widths but must be considered as much less precise values than those listed for **1a**, **2a**, and **3a**.

The ionization energies are substantially lowered by the presence of the Si and Sn moieties. For example, the HOMO ionization energy decreases in the series **1a** > **1b** > **1c** > **1d**. This is in accord with expectations because a better energy match of C−Sn than C−Si than C−C orbitals with p-type sulfur lone-pair orbitals should destabilize the HOMO following the
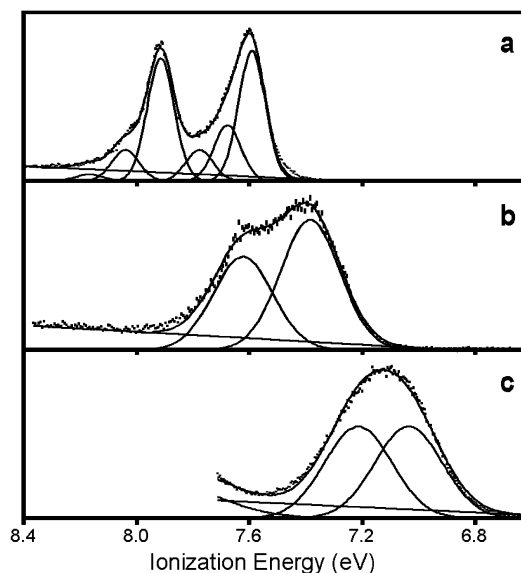
series C−Sn > C−Si > C−C (assuming comparable geometries). The destabilization is substantial, up to 0.8 eV (compare **1a** and **1d**). This same effect is observed in the selenium and tellurium analogues **2a−c** and **3a,b**, respectively, as seen in Table 1. Since the energy for a selenium 4p or tellurium 5p lone-pair orbital is lower than the energy of a sulfur 3p orbital, there is a poorer energy match between a selenium 4p or tellurium 5p orbital and C−Si or C−Sn orbitals than is expected for a sulfur 3p orbital and C−Si or C−Sn orbitals. Consequently, less destabilization of the first ionization energy is observed between these selenium or tellurium compounds than was observed between the corresponding sulfur compounds. The difference in the first ionization energies are 0.37 eV for **1a** versus **1b**, but only 0.29 eV for **2a** versus **2b** and 0.21 eV for **3a** versus **3b**, and 0.77 eV for **1a** versus **1d** but only 0.58 eV for **2a** versus **2c**.

The substantial lowering of the HOMO ionization energy of **3c** relative to **3a** (0.55 eV) is due to the Si−Si moieties in **3c**. This effect has been analyzed for **1e** previously as follows.[6] Calculations on model **8** in which θ and ϕ are the dihedral angles about the MeS−CSi and SC−SiSi bonds, respectively,

$$\text{MeS} \overset{\theta}{-} \text{CH}_2 \overset{\phi}{-} \text{SiMe}_2 - \text{SiMe}_3$$

8
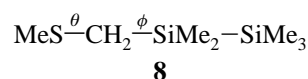
were done to understand sulfur lone pair, Si−Si interactions. When θ = 90° and ϕ = 180°, the geometry of **8** is optimized
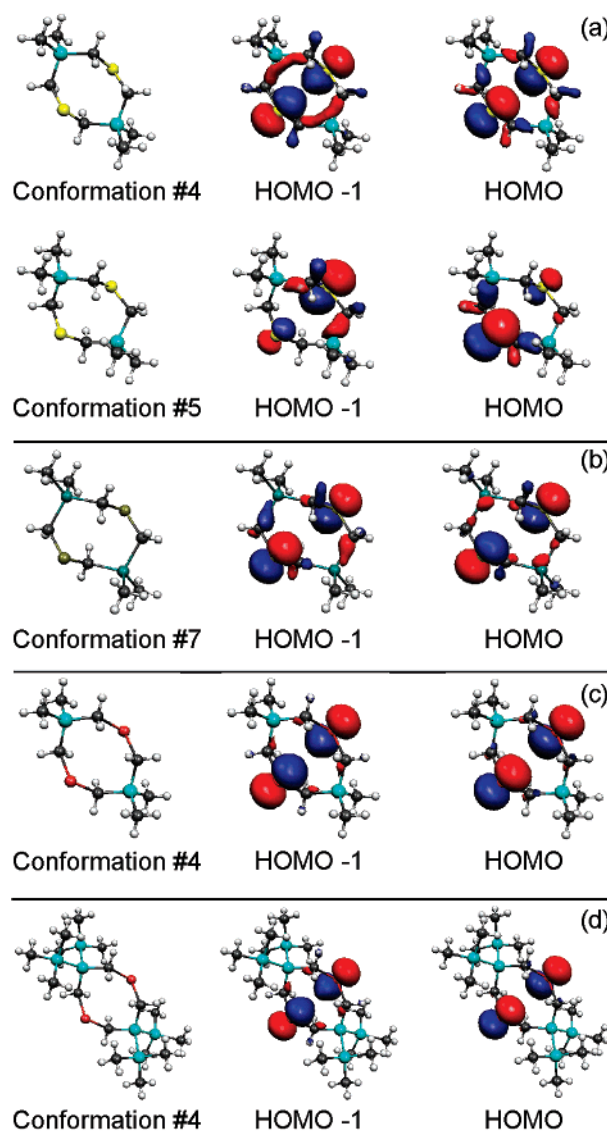
TABLE 2. Lowest Energy Conformational Minima Calculated (B3LYP/CEP-121G) for Selected Compounds

conformer	relative free energy (kcal/mol)	Boltzmann population	chalcogen lone pair ΔIE (eV)	chalcogen− chalcogen distance (Å)	through-space lone pair ΔIE (eV)
1b					
#4	0.000	0.501	0.16	3.873	0.52
#5	0.119	0.409	0.15	4.087	0.32
2c					
#7	0.000	0.501	0.05	4.616	0.19
3b					
#4	0.000	0.921	0.16	4.386	0.42
3c					
#4	0.000	0.999	0.17	4.256	0.51

for asymmetric combination of the sulfur p-orbital, C−Si and Si−Si σ-orbitals. Comparable interactions occur with **1e** because in the lowest energy conformation calculated for **1e** the dihedral angles are approximately $\theta = 119°$, $\phi = 163, 74°$. Molecular orbital calculations on this conformer reveal that its HOMO (and HOMO-1) is derived from all of the ring atoms and that the exocyclic Si−Si orbitals participate. That is, the combined geminal Si−Si orbitals interact with the sulfur lone-pair orbitals through the C−Si orbitals accounting for the destabilization observed. This same analysis has been extended to **3c** (see Table 2 and Figure 5) and accounts for the observed destabilization.

Although the experimental lone-pair orbital splittings in **1b−d**, **2b,c**, and **3b,c** are comparable, which could be consistent with similar geometries, the lone-pair splittings for these molecules do differ significantly from those for **1a**, **2a**, and **3a**. It is not clear from the experimental data alone if the differences in lone-pair orbital splittings between these two groups of molecules are due to the presence of the Si and/or Sn groups or due to conformational differences. Consequently, a theoretical conformational and orbital analysis of **1b**, **2c**, **3b**, and **3c** was performed. As pointed out previously,[12,14] the lone-pair orbital splitting as measured by PES can be compared to lone-pair orbital splittings from molecular orbital calculations to provide information about medium-sized ring polythioether conformations.

The conformational analysis of **1b** was carried out by selecting candidate conformations based on previously observed or calculated geometries for polythioethers,[15] which were then geometry optimized to obtain energy minima. Six conformations that are true energy minima and are within 6 kcal/mol of the lowest energy conformation were found. Molecular orbital calculations were then done for each of these conformations, and the two highest occupied MOs were plotted to aid in the analysis of their composition. The two lowest energy conformations of **1b** and plots of their two highest occupied MOs are shown in Figure 5a. Table 2 lists the relative energies of these two conformations, their calculated Boltzmann populations at 298.15 K, the nonbonded S···S distances, and the differences in energy calculated between the two highest occupied MOs (ΔIE). The comparable data for the other four conformations of **1b** are given in the Supporting Information. The conformation that is found in the solid state by X-ray crystallographic methods[5] is a boat,boat conformation (conformer #1), which is not that calculated to be the lowest energy conformer in the

(14) Setzer, W. N.; Glass, R. S. In *Conformational Analysis of Medium-Sized Heterocycles*; Glass, R. S., Ed.; VCH: Weinheim, Germany, 1988; Chapter 4.

(15) Clennan, E. L.; Hightower, S. E.; Greer, A. *J. Am. Chem. Soc.* **2005**, *127*, 11819−11826.

FIGURE 5. Lowest energy conformations and plots of their HOMO and HOMO-1 for (a) **1b**, (b) **2c**, (c) **3b**, and (d) **3c**.

gas phase (i.e., conformer #4). In addition, conformer #5 is calculated to be within 0.1 kcal/mol of the lowest energy conformer. These computational results suggest that there will be a mixture of conformers #4 and #5 in the gas phase, each contributing to the observed PES. Because the observed PES represents a composite of these conformations, the fitting of the spectrum shown in Figure 2b and consequent ΔIE listed in Table 1 must be regarded as tentative. The PES of **1b** supports the preference for conformations #4 and #5 in the gas phase because the observed ΔIE (0.20 eV) is close to that calculated for these conformers (0.16 eV for #4, 0.15 for #5), but not so close to that calculated for conformer #1 (0.04 eV).

Examination of the HOMO for conformation #4 reveals that it is the antisymmetric combination of the two p-type sulfur lone-pair orbitals that is further destabilized by π-type C−Si and C−H interactions. Such interactions are reminiscent of the reported π-CH$_2$ destabilization of the HOMO of thietane,[16] and mixing of sulfur 3p lone-pair orbitals with π-type molecular

(16) Mollere, P. D.; Houk, K. N. *J. Am. Chem. Soc.* **1977**, *99*, 3226−3233.
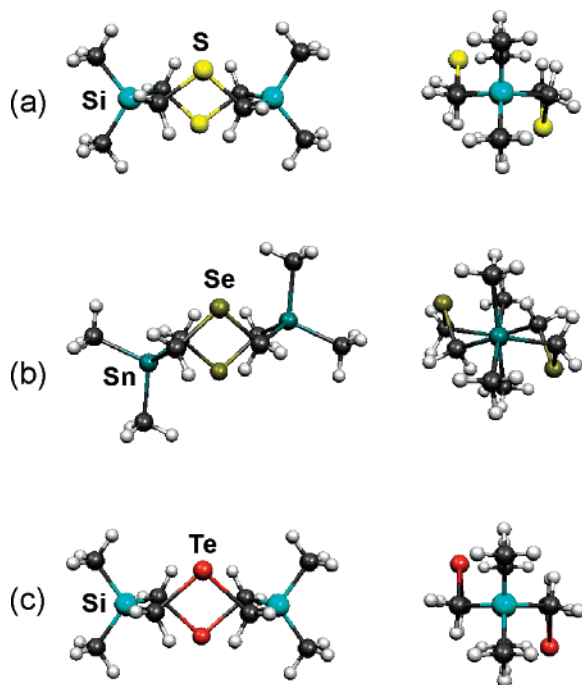
FIGURE 6. View of (a) **1b** conformer #4, (b) **2c** conformer #7, (c) **3b** conformer #4 down the C_2 axis and view along C—M—C edge down the chalcogen—chalcogen axis.

orbitals obtained by combining C—Si and C—H σ MOs has been reported before.[6] Similar destabilization also occurs with HOMO-1 of conformation #4, which is the symmetric combination of p-type lone-pair orbitals. Formation of this symmetric combination would be anticipated to be stabilizing energetically. However, destabilizing through-bond interaction between the lone-pair orbitals, mediated by the C—Si σ-orbitals in the ring, is clearly seen in the orbital plot. This through-bond interaction has the consequence of further raising the energy of HOMO-1. Similar interactions are present in the HOMO-1 of conformer #5. Thus, the modest ΔIE measured for this compound is due to additional destabilization of HOMO-1 by through-bond interaction. To provide more quantitative insight into this effect, the following was done. To estimate the ΔIE due solely to through-space interaction, two molecules of H_2S were placed in the same orientation and with the same nonbonded S···S distance as the CH_2SCH_2 moieties in each energy minimum conformer of **1b**. The results are listed in the Supporting Information as through-space ΔIE. For conformation #4, this value is 0.52 eV as opposed to the 0.16 eV ΔIE calculated for the entire molecule in this conformation, which demonstrates the importance of the through-bond interaction influence on the energy of HOMO-1 and the subsequent ΔIE for this conformer.

Geometry optimizations were performed on **2c** beginning at six geometries based on the energy minima calculated for **1b** but starting geometries #3, #4, and #5 optimized instead to a new conformation #7 that is calculated to be the most stable in the gas phase. This conformer is similar to conformer #4 of **1b** but with a twist about the C—Sn—C ring atom plane with respect to the other C—Sn—C ring atom plane that is presumably made preferable by the longer Se—C and Sn—C bonds so that the eclipsing strain is relieved. This twist is clearly seen by looking along the C—Sn—C edge of the ring down the Sn,Sn axis, as shown in Figure 6.

The lowest energy minimum conformation for **2c** is shown in Figure 5b, and the other conformations are shown in the Supporting Information. Three conformations are within 1 kcal/mol of each other and hence have similar Boltzmann populations; a mixture of conformers is expected in the gas phase, each contributing to the observed photoelectron spectrum. In the solid state, **2c** adopts a twist-chair conformation,[5] with a C_2 axis through the Sn atoms as shown by X-ray crystallography, which corresponds to conformer #1 (see Supporting Information).

The two highest energy occupied MOs for the lowest energy conformation of **2c** are plotted in Figure 5b, and those for the others are found in the Supporting Information. Again, π-like C—Sn/C—H interactions destabilize the p-type selenium lone-pair orbitals. As experimentally measured, the consequence of the destabilization is that the lowest ionization energy for **2c** is lowered compared with **2a**. In addition, comparison of the experimentally observed ΔIE with the calculated ΔIE for the model in which through-bond interaction is excluded (i.e., the model in which two H_2Se molecules occupy the CH_2SeCH_2 positions with the same orientation as in each conformer) shows large through-bond effects for conformations #7 and #2. Indeed, the through-bond interactions are so predominant that the symmetric lone-pair combination, usually HOMO-1 for medium-sized ring dichalcogenides, is now the HOMO for conformation #7, which is calculated to be the most stable conformer in the gas phase.

The lowest energy conformer found computationally for **3b** is shown in Figure 5, and the other conformers are given in the Supporting Information. For **3b**, the longer Te—C bonds combined with the shorter C—Si bonds apparently destabilize both **1b** conformation #5 and the **2c** conformation #7; as a consequence, **1b** conformation #5 optimized to conformation #4 for **3b**. The lowest energy conformer is #4 (C_2 symmetry), which corresponds to that found in the solid state by X-ray crystallography,[5] and is calculated to be substantially lower in energy than the other conformations. Hence, the observed photoelectron spectrum of **3b** likely corresponds to only this conformer. It is interesting to note that the photoelectron spectrum of **3b** does contain more structure than those of **1b** or **2c**, which would agree with the presence of only one conformation of **3b** in the gas phase. This conformation is analogous to the lowest energy conformer found computationally for the analogous sulfur compound **1b**. The two highest occupied MOs for conformation #4 of **3b** are shown in Figure 5, and those for the other conformers are shown in the Supporting Information. For each conformer, these orbitals are very similar to those found for the corresponding conformer of **1b**. The separation of HOMO and HOMO-1 calculated for the lowest energy conformer of **3b** (0.16 eV) is close to the experimental value (0.24 eV).

The lowest energy conformer of **3c** found computationally and its two highest MOs are shown in Figure 5d, and those for the other conformers can be found in the Supporting Information. The conformation that would correspond to conformer #6 of the other molecules studied here would be extremely unstable due to near superposition of methyl groups of the $SiMe_3$ moieties. Therefore, for **3c**, this conformation was eliminated. The remaining five conformations were optimized. As was the case for **3b**, conformation #5 optimized to #4. These calculations showed that conformation #4 is the lowest energy conformation by such a significant amount that only this conformation is

expected to be present in the gas phase.[17] The calculated lone-pair splitting of 0.17 eV agrees with the experimentally determined value of 0.17 eV. Furthermore, the MOs of conformer #4, while of predominantly lone-pair character, are derived from orbitals of all of the ring atoms as well as the exocyclic Si–Si orbitals. These combined geminal Si–Si orbitals interact with the tellurium lone-pair orbitals through the C–Si orbitals. This extended interaction accounts for the substantial destabilization of these orbitals.

Conclusion

For the series of mixed group 14 and 16 heterocycles studied, CT spectroscopy provides a good indicator of their lowest ionization energies. These energies are lowered by interaction of C–Si, C–Sn, and Si–Si σ-bonds with S, Se, and Te lone pairs in a geometry-dependent way. Theoretical calculations revealed the basis for these interactions. Those interactions may render the chalcogens better n-donors in complexation with metals and the heterocycles better donor components in electrically conducting materials.

Experimental Section

Charge-Transfer Spectroscopy. A solution of the complexes in CH_2Cl_2, which was distilled from P_2O_5 under nitrogen, was made using a 1:1 molar ratio of heterocycle to multiply recrystallized TCNE, and a concentration between 1 and 9 mM.

Photoelectron Spectroscopy. Gas-phase photoelectron spectra were recorded using an instrument that features a 36 cm, 8 cm gap hemispherical analyzer and custom designed sample cells and discharge source. Electron detection and instrument control are provided through custom software interfaced to a multifunction DAQ board. The ionization energy scale was calibrated using the $^2E_{1/2}$ ionization of methyl iodide (9.538 eV), with Ar $^2P_{3/2}$ ionization (15.759 eV) used as an internal energy scale lock during data collection. During data collection, the instrument resolution, measured using the full-width at half-maximum of the Ar $^2P_{3/2}$ ionization, was 0.015–0.025 eV. All data are intensity-corrected with an experimentally determined instrument analyzer sensitivity function that assumes a linear dependence of analyzer transmission (intensity) to the kinetic energy of the electrons within the energy range of these experiments. The He I spectra were corrected for ionizations from He Iβ photons (1.9 eV higher in energy, and 3% the intensity of the He Iα photons).[18]

The samples were cooled and loaded into a sample cell that had been cooled in a −40 °C freezer for 15–45 min. The cell was then placed in the instrument and allowed to slowly warm, and the spectra were collected at the temperature (monitored using a "K"-type thermocouple passed through a vacuum feedthrough and attached directly to the sample cell) where sufficient sample vapor pressure was achieved.

Data Analysis. In the figures of the data, the vertical length of each data mark represents the experimental variance of that point.[19] The valence ionization bands are represented analytically with the best fit of asymmetric Gaussian peaks.[19] The bands are defined with the position, amplitude, and half-width for the high binding energy side of the peak, and the half-width for the low binding energy side of the peak. The peak positions and half-widths are reproducible to about ±0.02 eV (∼3σ level). Confidence limits for the relative integrated peak areas are about 5%, with the primary source of uncertainty being the determination of the baseline, which is caused by electron scattering and taken to be linear over the small energy range of these spectra. The total area under a series of overlapping peaks is known with the same confidence, but the individual peak areas are more uncertain. The fitting procedures used are described in more detail elsewhere.[19]

Computational Methodology. Calculations were performed with Gaussian 03 (rev. B.04 under Mac OS X or C.02 under IBM AIX).[20] All computations were carried out using Becke's three-parameter hybrid method with Perdew and Wang's exchange-correlation functional (B3PW91).[21] All computations were carried out using the CEP-121G split-valence basis set with effective core potentials.[22,23] Geometries were optimized, and the frequencies of the optimized geometries were computed to verify that there were no imaginary frequencies. Vertical ionization potentials were computed by the ΔSCF method (total difference between the cation radical energy at the neutral minimized geometry and the neutral energy at that geometry), but orbital energies were estimated from the orbital eigenvalues (by a modification of Koopmans' theorem; see below); the vertical IPs are therefore expected to be more reliable than the orbital energies. The method which was used to estimate most of the orbital energies takes the difference between the HOMO eigenvalue and the orbital eigenvalue and adds this to the computed molecular vertical IP (essentially constituting an offset correction to the normal Koopmans' theorem values). Orbital plots were created using the visualization program Molekel 4.3.win32 with a surface value of 4%.[24]

(17) As reported in ref 6, interactions in MeSCSiSi moieties are governed by two geometrical parameters: the dihedral angle θ about the MeS–CSi bond and the dihedral angle ϕ about the SC–SiSi bond. The dihedral angles about the CTe–CSi bond (θ) and TeC–SiSi bond (ϕ) in **3c** are 116 and 70, and 170°, respectively. These dihedral angles are comparable to those found for **1e**.

(18) Turner, D. W.; Baker, C.; Baker, A. D.; Brundle, C. R. *Molecular Photoelectron Spectroscopy*; Wiley-Interscience: London, 1970.

(19) Lichtenberger, D. L.; Copenhaver, A. S. *J. Electron Spectrosc. Relat. Phenom.* **1990**, *50*, 335–352.

(20) Frisch, M. J.; Trucks, G. W.; Schlegel, H. B.; Scuseria, G. E.; Robb, M. A.; Cheeseman, J. R.; Montgomery, J. A., Jr.; Vreven, T.; Kudin, K. N.; Burant, J. C.; Millam, J. M.; Iyengar, S. S.; Tomasi, J.; Barone, V.; Mennucci, B.; Cossi, M.; Scalmani, G.; Rega, N.; Petersson, G. A.; Nakatsuji, H.; Hada, M.; Ehara, M.; Toyota, K.; Fukuda, R.; Hasegawa, J.; Ishida, M.; Nakajima, T.; Honda, Y.; Kitao, O.; Nakai, H.; Klene, M.; Li, X.; Knox, J. E.; Hratchian, H. P.; Cross, J. B.; Bakken, V.; Adamo, C.; Jaramillo, J.; Gomperts, R.; Stratmann, R. E.; Yazyev, O.; Austin, A. J.; Cammi, R.; Pomelli, C.; Ochterski, J. W.; Ayala, P. Y.; Morokuma, K.; Voth, G. A.; Salvador, P.; Dannenberg, J. J.; Zakrzewski, V. G.; Dapprich, S.; Daniels, A. D.; Strain, M. C.; Farkas, O.; Malick, D. K.; Rabuck, A. D.; Raghavachari, K.; Foresman, J. B.; Ortiz, J. V.; Cui, Q.; Baboul, A. G.; Clifford, S.; Cioslowski, J.; Stefanov, B. B.; Liu, G.; Liashenko, A.; Piskorz, P.; Komaromi, I.; Martin, R. L.; Fox, D. J.; Keith, T.; Al-Laham, M. A.; Peng, C. Y.; Nanayakkara, A.; Challacombe, M.; Gill, P. M. W.; Johnson, B.; Chen, W.; Wong, M. W.; Gonzalez, C.; Pople, J. A. *Gaussian 03*, revision C.02; Gaussian, Inc.: Wallingford, CT, 2004.

(21) Becke, A. D. *J. Chem. Phys.* **1993**, *98*, 5648–5652.

(22) (a) Stevens, W. J.; Basch, H.; Krauss, M. *J. Chem. Phys.* **1984**, *81*, 6026–6033. (b) Stevens, W. J.; Krauss, M.; Basch, H.; Jasien, P. G. *Can. J. Chem.* **1992**, *70*, 612–630. (c) Cundari, T. R.; Stevens, W. J. *J. Chem. Phys.* **1993**, *98*, 5555–5565.

(23) Support that this computational method adequately describes the compounds reported in this paper can be found in ref 6.

(24) (a) Flükiger, P.; Lüthi, H. P.; Portmann, S.; Weber, J. *MOLEKEL 4.3*; Swiss Center for Scientific Computing, Manno, Switzerland, 2000–2002. (b) Portmann, S.; Lüthi, H. P. *Chimia* **2000**, *54*, 766–769.

(25) (a) Petrukhina, M. A.; Henck, C.; Li, B.; Block, E.; Jin, J.; Zhang, S.-Z.; Clerac, R. *Inorg. Chem.* **2005**, *44*, 77–84. (b) Block, E.; Dikarev, E. V.; Jin, J.; Li, B.; Petrukhina, M. A.; Zhang, S.-Z. *Pure Appl. Chem.* **2005**, *77*, 2029–2932.

(26) Stein, C. A.; Lewis, N. A.; Seitz, G.; Baker, A. D. *Inorg. Chem.* **1983**, *22*, 1124–1128.

(27) Dikarev, E. V.; Shpanchenko, R. V.; Andreini, K. W.; Block, E.; Jin, J.; Petrukhina, M. A. *Inorg. Chem.* **2004**, *43*, 5558–5563.

(28) Traven, V. F.; Rokitskaya, V. I.; Rodin, O. G.; Shvets, A. F.; Redchenko, V. V.; Voronkov, M. G.; Kirpichenko, S. V.; Suslova, E. N. *Dokl. Akad. Nauk SSSR* **1986**, *288*, 1160–1163.

Supporting Information Available: Table of calculated conformational minima for **1b**, **2c**, **3b**, and **3c**; figures of conformational minima plots of the HOMO and HOMO-1 for **1b**, **2c**, **3b**, and **3c**; Cartesian coordinates for conformational minima calculated for **1b**, **2c**, **3b**, and **3c**; Cartesian coordinates of the H_2E dimers used to model chalcogen through-space interactions for **1b**, **2c**, **3b**, and **3c**. This material is available free of charge via the Internet at http://pubs.acs.org.

JO071215V